Icarus xxx (xxxx) xxxx

Contents lists available at ScienceDirect

Icarus

journal homepage: www.elsevier.com/locate/icarus

Titan's neutral atmosphere seasonal variations up to the end of the Cassini mission

A. Coustenis[a,*], D.E. Jennings[b], R.K. Achterberg[b,c], P. Lavvas[d], G. Bampasidis[e], C.A. Nixon[b], F.M. Flasar[b]

[a] Laboratoire d'Etudes Spatiales et d'Instrumentation en Astrophysique (LESIA), Observatoire de Paris, CNRS, Université Paris-Science-et-Lettres, Sorbonne Université, Université de Paris, 5, place Jules Janssen, 92195 Meudon Cedex, France
[b] Detector Systems Branch, Goddard Space Flight Center, Greenbelt, MD 20771, USA
[c] Department of Astronomy, University of Maryland, College Park, MD 20742, USA
[d] Université de Reims Champagne-Ardennes, CNRS, GSMA, UMR 7331, 51097 Reims, France
[e] School of Education, Department of Primary Education, National & Kapodistrian University of Athens, 10680 Athens, Greece

ARTICLE INFO

Keywords:
Titan
Titan, atmosphere
Satellites, atmospheres
Spectroscopy
Radiative transfer

ABSTRACT

In this paper we report new results concerning the seasonal atmospheric evolution near Titan's poles and equator in terms of temperature and composition using nadir spectra acquired by the Cassini Composite Infrared Spectrometer (CIRS) at high spectral resolution during the last year of the Cassini mission in 2017 complementing previous investigations covering almost two Titan seasons. In recent previous papers (Coustenis et al., 2016, 2018), we have reported on monitoring of Titan's stratosphere near the poles after the mid-2009 northern spring equinox. In particular we have reported on the observed strong temperature decrease and compositional enhancement above Titan's southern polar latitudes since 2012 and until 2014 of several trace species, such as complex hydrocarbons and nitriles, which were previously observed only at high northern latitudes. This effect accompanied the transition of Titan's seasons from northern winter in 2002 to northern summer in 2017, while at that latter time, the southern hemisphere was entering winter. Our new data, acquired in 2017 and analyzed here, are important because they are the only ones recorded since 2014 close to the south pole in the mid-infrared nadir mode at high resolution. A large temperature increase in the southern polar stratosphere (by 10–50 K in the 0.1 mbar–0.01 mbar pressure range) is found associated with a change in the temperature profile's shape. The 2017 observations also show a related significant decrease in most of the southern abundances which must have started sometime between 2014 and 2017. For the north, the spectra indicate a continuation of the decrease of the abundances which we first reported to have started in 2015 and small temperature variations. We discuss comparisons with other results and with current photochemical and dynamical models which could be updated and improved by the new constraints set by the findings presented here.

1. Introduction

The Cassini-Huygens mission observed the Saturnian system for 13 years, covering about two Saturnian seasons and providing a wealth of data which yield considerable new information about the objects in the system. Among the kronian satellites, Titan offered the opportunity for many new discoveries in its system where the atmosphere, the surface and the interior are interconnected and evolve with the season (from early winter in the north at the beginning of the mission in mid-2004, until its end just after summer solstice in mid-2017). The last targeted Titan flyby was on April 23, 2017, in the beginning of Cassini Grand Finale orbits when the spacecraft started dipping between the rings and the planet. The last non-targeted Titan flyby was on September 11, 2017 putting Cassini on impact trajectory with Saturn. Among other, the atmospheres of the planet itself and Titan have been investigated by the Cassini Composite Infrared Spectrometer (for the description of CIRS see for instance Flasar et al., 2004 and Jennings et al., 2017). The data we present here pertain to the stratosphere of Titan, above the poles and near the equator as observed from different trajectory points in 2017 within the Grand Finale mission.

* Corresponding author at: Laboratoire d'Etudes Spatiales et d'Instrumentation en Astrophysique (LESIA), Observatoire de Paris, CNRS, PSL Univ., Sorbonne Univ., Paris Univ., 5, place Jules Janssen, 92195 Meudon Cedex, France.
E-mail address: athena.coustenis@obspm.fr (A. Coustenis).

https://doi.org/10.1016/j.icarus.2019.113413
Received 11 March 2019; Received in revised form 6 August 2019; Accepted 13 August 2019

Several investigators have found variations in temperature and composition within Titan's stratosphere both in a spatial and a temporal distribution. Seasonal variations from CIRS data obtained during the duration of the Cassini mission were reported in numerous previous publications by this team and other authors (e.g. Coustenis et al., 2007, 2010, 2013; Teanby et al., 2012, Teanby et al., 2017; Vinatier et al., 2015, Vinatier et al., 2018; Jennings et al., 2012a). This team has recently focused on analyses of spectra acquired near polar latitudes by Cassini/CIRS at high resolution in the 600–1500 cm^{-1} range to infer the composition and temperature of Titan's stratosphere probed at those wavenumbers (Coustenis et al., 2016, 2018). In particular, fast and important seasonal effects have been observed in the atmosphere of the satellite pointing to a large-scale reversal, which occurred in the single pole-to-pole circulation of Titan's atmosphere after the northern equinox in mid-2009 and which led to gases upwelling from the southern summer hemisphere and then downwelling at the northern winter pole (Achterberg et al., 2008, Achterberg et al., 2011; Teanby et al., 2012; Bampasidis et al., 2012), significantly affecting the temperature and the composition near the poles of Titan. It is noteworthy that all previous investigations indicate that the polar and mid-latitude abundances show different trends indicating different dynamical processes which occur inside and out of the polar vortex region, extending down to about 50°S in latitude.

While most trace stratospheric gases in the north polar data generally show only a small decreasing trend until 2014, the southern polar results on the contrary point to a strong enhancement after 2012 (Coustenis et al., 2016, 2018). As argued also by other investigators (e.g. Vinatier et al., 2015; Teanby et al., 2017), this indicates a fast and strong buildup of the gases in the southern pole while it goes deeper into the shadow during the 2013–2014 southern autumn, as predicted by models (e.g. Hourdin et al., 2004; Rannou et al., 2005; Lebonnois et al., 2009, 2012). This was associated with temperature changes we have registered in our previous publications where from 2013 until 2016, the northern polar region has shown a temperature increase of 10 K, while the south has shown a more significant decrease (up to 25 K) in a similar period of time. Jennings et al. (2012a, 2012b, 2015) found that the increase in gaseous content in the south is related to the haze increase that was also seen in the south following its decrease in the north. As indicated in these previous publications, after northern spring equinox in 2009, we discovered that the global dynamics in Titan's atmosphere changed dramatically. Seasonal solar heating moved towards the north pole, where the vortex began weakening, as indicated by the decrease in the equator-to-pole temperature gradient. At the same time, in the south pole a hot spot was formed in the higher northern polar stratosphere leading to a large enrichment of trace gaseous components, aerosols and condensates produced by photochemistry (West et al., 2011, 2016; Jennings et al., 2012a, 2012b, 2015; Coustenis et al., 2013; Teanby et al., 2017; Vinatier et al., 2015, Vinatier et al., 2018). Thus, towards the end of that period, the strong gaseous signatures had almost disappeared in the north, and similar features started to appear near the south polar stratosphere which evolved with the season there heading towards winter.

The new 2017 stratosphere data we present here consist of eight selections in FP3 and FP4 above Titan's north pole at latitudes between 65°N and 90°N and six selections above the south pole beyond 65°S. We have also analyzed a large spectral average around the equator. The selections are described in Table 1. This paper then follows the Coustenis et al. (2016 and 2018) publications on seasonal effects in the atmosphere, looking for the predicted and theorized changes in abundance of the polar constituents. In Section 2 we describe our data and stress the importance of the selections in 2017 that we analyze here, but we also include results from years after 2010. We also briefly describe the method used in the analysis that has been applied to previous publications. Section 3 we present our results and discuss the context within original and intriguing changes in the trends for the atmospheric temperature and chemical structure are observed importantly complementing the previous findings. In Section 4 we conclude and compare with existing photochemical and general circulation models (GCM) pointing at constraints that could be useful in updating and improving them.

2. Observations and data analysis

The data analyzed in this article were taken in 2017 by CIRS at high spectral resolution (0.5 cm^{-1}) in the surface-intercepting nadir mode. The Cassini CIRS instrument is described in Flasar et al. (2004) and Jennings et al. (2017). It consists of a Fourier transform spectrometer operating in the 10 to 1500 cm^{-1} spectral range, divided in three channels or Focal Planes (FP). Titan observations with CIRS during the Cassini mission are described extensively in Nixon et al. (2019). Here, we use the spectra acquired in the mid-infrared focal planes (FP3 and FP4) that cover the 600–1500 cm^{-1} range. CIRS spectra in this spectral range probe the stratosphere which covers levels between roughly 100 and 400 km in altitude and pressure levels between 0.01 and 20 mbar essentially for the CIRS nadir polar observations (Flasar et al., 2005).

In particular, since we require high-resolution nadir spectra of Titan's stratosphere near the poles (from 65° to 90°), in order to separate the contributions of the different gas components (see for example Coustenis et al., 2010), we have to point out that this type of dataset suffers occasionally from lack of observations for high latitudes, caused by Cassini's orbital geometry (see Fig. 1 in Coustenis et al., 2018 and also Nixon et al., 2019). Indeed, the north pole was not observed before mid-2013 and between fall 2014 and May 2016. For the south pole we did not have enough high-resolution (0.5 cm^{-1}) available spectra from fall of 2014 onwards and until 2017. The 2017 data that we present here are then very important because they give us for the first time an indication to what happened in the south polar stratosphere after 2014 and because they increase the number of observations we can analyze in the northern pole region.

Fig. 1 shows a comparison between the more recent (2017) CIRS spectra and the 2014 ones in the 1100–1400 cm^{-1} range (FP4 focal plane, where the methane band is located) hinting to strong changes having occurred since that time close to the South Pole. Indeed, a strong increase in the emission in the CH_4 band in 2017 corresponds to a much hotter stratosphere in these later dates as will be quantified below. See Fig. 2 of Coustenis et al. (2016) for indications of gradual enhancement in Titan's south pole atmosphere from the FP3 spectra.

Table 1 shows the spectra used in this work for complementing our monitoring of the temporal and seasonal evolution of Titan's polar thermal and chemical stratospheric structure, in particular since 2012. In addition, we have included a large spectral average near the equator in order to compare with previous inferences.

The field of view (FOV) of our CIRS observations was restricted to be entirely on Titan's disk and emission angles were limited to 0–65° to avoid the need for large atmospheric corrections. Available spectra within each time period were zonally averaged in large latitude bins covering latitudes within the 65° to 90° latitude range. The averages depend on the data available for a given date/flyby within a latitude range and aim at improving the signal-to-noise ratio (except for the equatorial average which spans several dates from February to September 2017).

All of the 2017 spectral averages in Table 1 include spectra between 65°S and 90°S with emission angles from 50 to 60° and most of the spectra corresponding to 70°S. We have two datasets near Titan's south pole in February 2017, one averaging data centered at 70°S and the other southern average with spectra from 70°S-90°S and emission angles from 30 to 60 degrees (with a much larger (10 times) total number of spectra included), being more representative of higher latitudes around 80°S.

As in previous papers, we use a monochromatic radiative transfer code adapted to Titan's stratosphere (ARTT: Coustenis et al., 2010; Bampasidis et al., 2012). Updates are included in Coustenis et al. (2010)

Table 1
This table shows the high resolution data taken in nadir mode near the south and north poles of Titan in focal planes 3 and 4 of the CIRS instrument. Ls is the solar longitude at the time of the observation. The distance to the satellite from the spacecraft is up to 400,000 km. In our previous papers, we refer to specific Titan close flybys in our selection tables. In this paper, we model CIRS spectra acquired from distant Titan flybys during Cassini Grand Finale mission and we use the COMPMAP parameter to identify them.

Year	Month	Latitudinal bin	Number of spectra	Airmass	COMPMAP	Ls (°)
FP3 spectral selections						
South pole						
2017	February	70°S to 90°S	1505	1.423	CIRS_259TI_COMPMAP001_PIE CIRS_259TI_COMPMAP002_PRIME	87
2017	February	68°S to 70°S	151	1.231	CIRS_259TI_COMPMAP001_PIE CIRS_259TI_COMPMAP002_PRIME	87
2017	June	65°S to 90°S	228	1.798	CIRS_280TI_COMPMAP001_PIE	91
North pole						
2017	February	65°N to 90°N	868	1.094	CIRS_261TI_MIDIRTMAP001_PRIME	87
2017	July	65°N to 90°N	2694	1.244	CIRS_283TI_COMPMAP001_PRIME CIRS_283TI_COMPMAP002_PRIME CIRS_283TI_COMPMAP003_PRIME	91
2017	August	65°N to 90°N	6667	1.249	CIRS_288TI_COMPMAP002_PIE CIRS_288TI_COMPMAP003_PIE	92
2017	September	65°N to 90°N	1920	1.222	CIRS_292TI_COMPMAP001_PRIME CIRS_293TI_COMPMAP002_PRIME	93
Equator						
2017	Feb-Sept	10°S to 10°N	902	1.218	[a]	87–93
FP4 spectral selections						
South pole						
2017	February	70°S to 90°S	1505	1.423	CIRS_259TI_COMPMAP001_PIE CIRS_259TI_COMPMAP002_PRIME	87
2017	February	68°S to 70°S	151	1.231	CIRS_259TI_COMPMAP001_PIE CIRS_259TI_COMPMAP002_PRIME	87
2017	June	65°S to 90°S	231	1.793	CIRS_280TI_COMPMAP001_PIE	91
North pole						
2017	February	65°N to 90°N	825	1.102	CIRS_261TI_MIDIRTMAP001_PRIME	87
2017	July	65°N to 90°N	2707	1.247	CIRS_283TI_COMPMAP001_PRIME CIRS_283TI_COMPMAP002_PRIME CIRS_283TI_COMPMAP003_PRIME	91
2017	August	65°N to 90°N	7089	1.222	CIRS_288TI_COMPMAP002_PIE CIRS_288TI_COMPMAP003_PIE	92
2017	September	65°N to 90°N	1935	1.190	CIRS_292TI_COMPMAP001_PRIME CIRS_293TI_COMPMAP002_PRIME	93
Equator						
2017	Feb-Sept	10°S to 10°N	975	1.168	[a]	87–93

[a] Our equatorial selections are spectral averages from all the datasets mentioned here in polar latitudes.

and more recent publications and the method is extensively explained in detail in Section 3 of Coustenis et al. (2007). In brief, we use a line-by-line radiative transfer code to simulate the observed Titan spectrum in FP3 and FP4 and through iterative processes we derive the temperatures and the abundances of the various constituents observe in Titan's atmosphere. We infer the temperature profile from the best fit of the 7.7-micron methane band in FP4 (following the method described in e.g. Achterberg et al., 2008) which performs inversions of the emission observed in the ν_4 methane band assuming 1.48% of CH_4 in the stratosphere increasing below the cold trap to about 5% at the surface as measured by the Huygens Gas Chromatograph Mass Spectrometer (GCMS) and compatible with the CIRS inferences from FP1 (Flasar et al., 2005; Niemann et al., 2010). The spectral modelling method for the temperature retrievals is described in Achterberg et al. (2008). Temperatures are retrieved using the constrained linear inversion algorithm of Conrath et al. (1998) using the spectral range from 1251 to 1311 cm^{-1} within the ν_4 band of methane. The methane absorption is calculated using the correlated-k approximation (Lacis and Oinas, 1991) with methane absorption data from HITRAN 2012.

Fig. 2 shows the fitting of the methane ν_4 band in the 1250 to 1350 cm^{-1} region. In our model the temperature profile is originally set to the one measured by CIRS emission values in the 7.7 μm CH_4 band and from lower resolution observations and then inverted to fit the FP4 spectrum (Achterberg et al., 2008, 2011; Coustenis et al., 2007, 2010, 2016; Bampasidis et al., 2012).

We then inject the temperature profile in our ARTT radiative transfer code and solve for the opacity in the rest of the spectrum retrieving the abundances of trace gases and their isotopes in the FP3 region of the CIRS spectra (for a full list of molecules included in our simulations and the associated spectroscopic parameters see previous publications and Table 2 in Jennings et al., 2017). Fig. 3 shows two of our fits in the 600–1000 cm^{-1} range, where we observe the emission of several gaseous bands of hydrocarbons, nitriles and oxygen compounds (e.g. HCN, C_2H_2, C_3H_8, C_2H_6, CO_2). We apply constant-with-height vertical profiles from the higher levels of the atmosphere (around 400 km in altitude) down to the condensation level and then follow the saturation curve. Our spectra were taken in the nadir mode and we lack information on the altitude dependence of the mixing ratios. This assumption is essentially valid for all the molecules considered here, due to their weak emission bands, except for C_2H_2 whose abundance variations with height are taken into account by making use of weighted averages over the P, Q and R branches of the 729 cm^{-1} band and by testing vertical profiles as described in detail in Bampasidis et al. (2012). We then infer mixing ratios that are constant-with-height above the condensation level and correspond to the atmospheric pressure levels indicated by the contribution functions in Fig. 4.

The uncertainty on our inferences is determined as explained in previous publications and in particular in Coustenis et al. (2010) and Bampasidis et al. (2012) with details. The uncertainties due to the measurements noise is small because the NESR (Noise Equivalent Spectral Radiance) is generally on the order of some 10^{-9} as shown in Fig. 23 of Jennings et al. (2017) for our spectral range, which combined

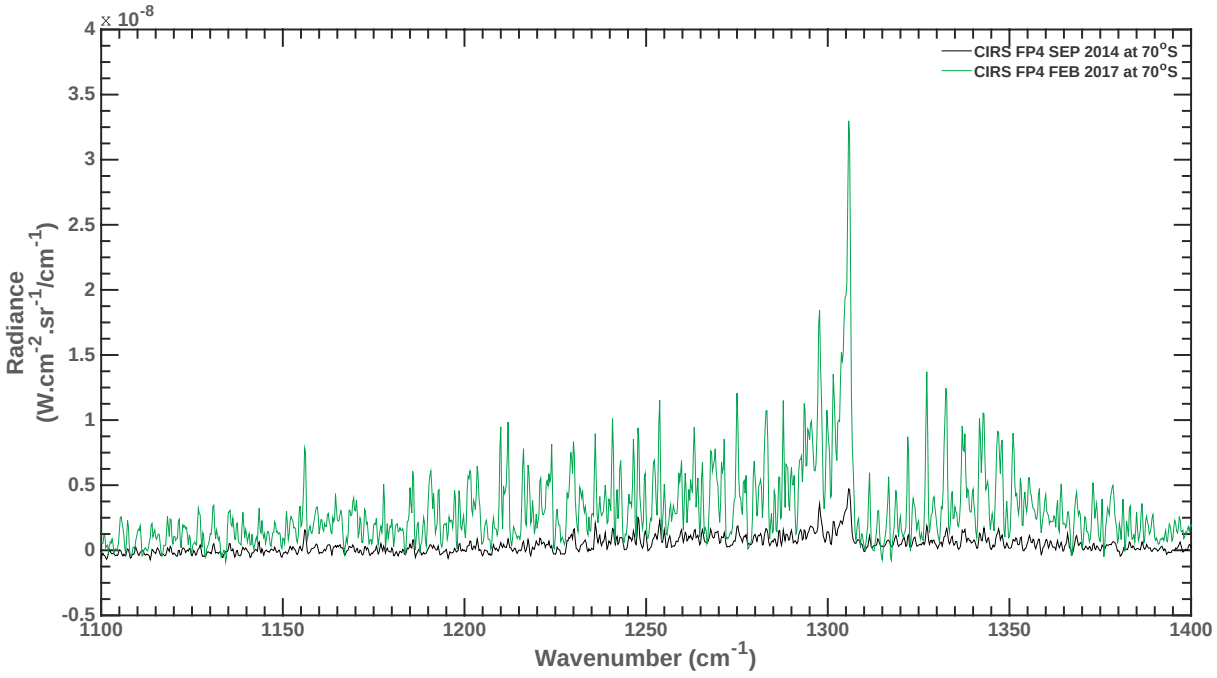

Fig. 1. comparison between September 2014 (black lines) and February 2017 (green lines) CIRS nadir spectra in the FP4 at high southern latitudes. The strong emission at 1304 cm^{-1} is due to the Q-branch of methane, and the peak at 1161 cm^{-1} is due to CH_3D. The September 2014 70°S data contain an average of 1187 spectra with an airmass of 1.2, the Feb 2017 70°S average has 151 spectra summed up for an airmass of 1.23, so the two datasets are at similar geometry conditions and can be compared. The differences indicate at a glance considerably stronger emission in the center and the wings of the CH_4 band in 2017 which is indicative of much higher temperatures in the south with respect to 2014. The purpose of the present work is to quantify such seasonal changes in temperature and composition. In this Figure and the following ones of this type, we restrain the longer wavenumber range to 1400 cm^{-1} for clarity purposes and because no exploitable information was retrieved here from the emission beyond that. (For interpretation of the references to colour in this figure legend, the reader is referred to the web version of this article.)

to the large number of spectra summed, gives noise levels of some 2 to 4 orders of magnitude smaller than the radiance in our averaged spectra. Thus, we take into account, as before, uncertainties due only to continuum fitting, temperature inferences and calibration.

3. Results and discussion

In our recent publication (Coustenis et al., 2018), we inferred the temperature profiles and the chemical composition at different dates from 2012 and up to 2016 for high northern and southern latitudes (at

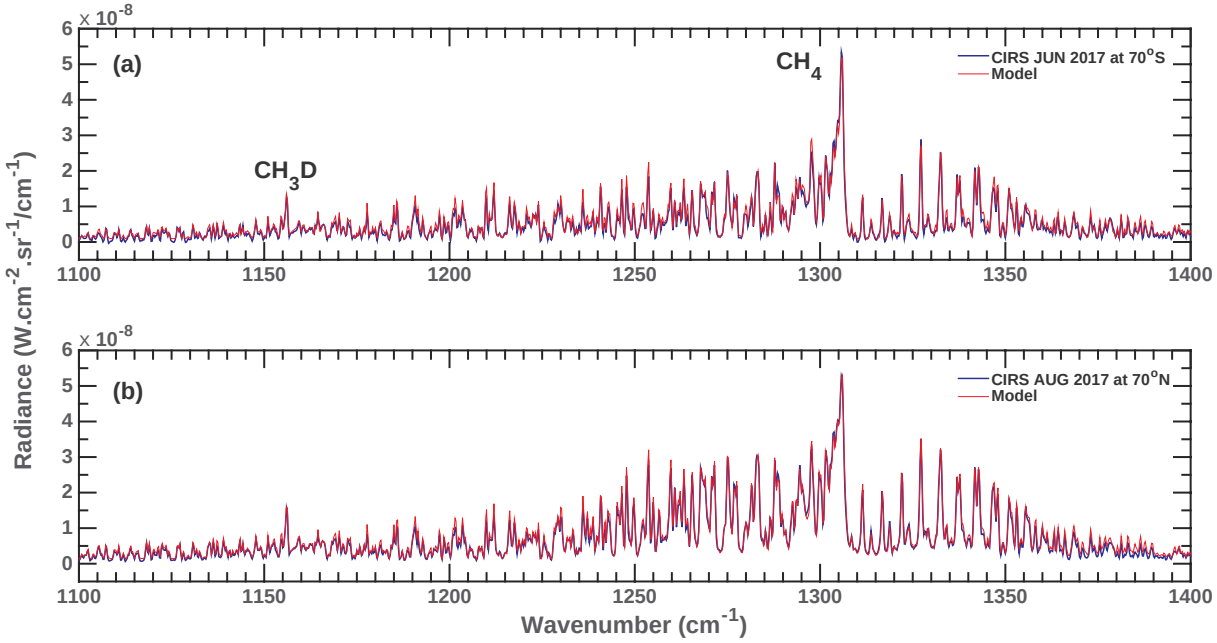

Fig. 2. Sample of fits in the 1200–1400 cm^{-1} part (FP4) of the Titan spectrum containing the CH_4 emission band at 7.7 μm which gives access to the temperature profile in the stratosphere. The blue curves are the CIRS observations in August 2017 at 75°N (top) and June 2017 at 70°S (bottom) and the red curves are the model simulations that best fit the data. (For interpretation of the references to colour in this figure legend, the reader is referred to the web version of this article.)

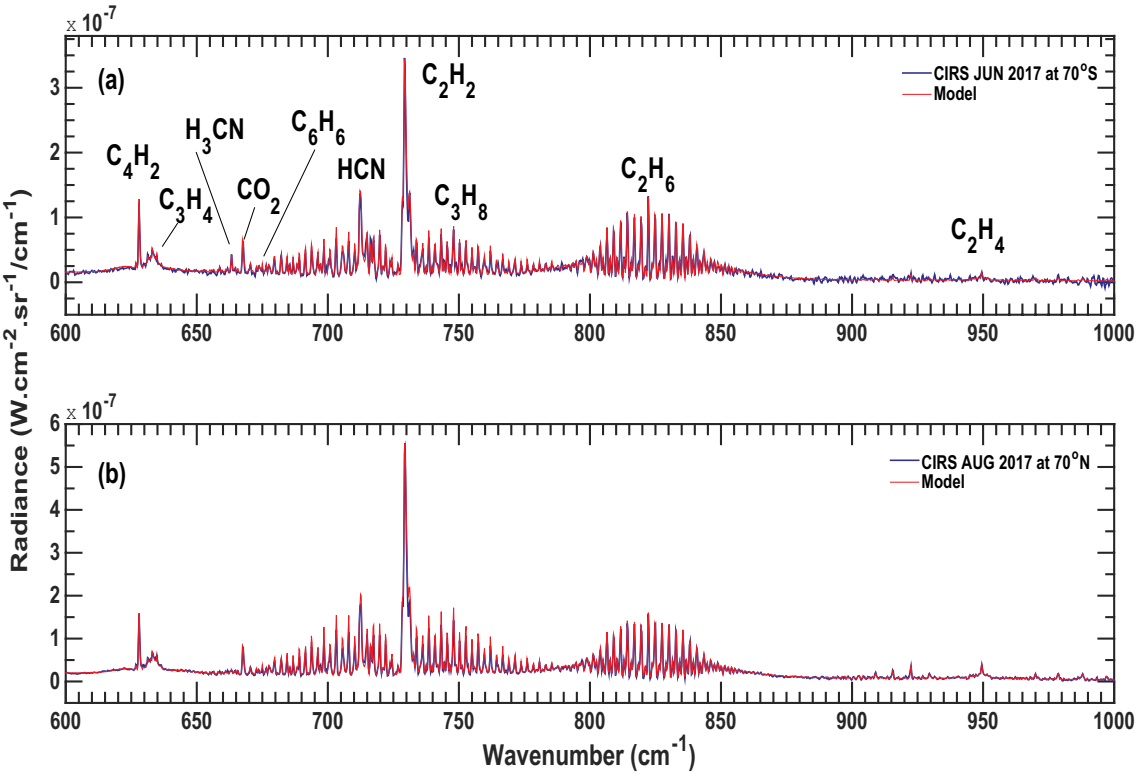

Fig. 3. Same as Fig. 2, but for a sample of fits in the 600–1000 cm^{-1}, part of the FP3 Titan spectrum, where the spectral signatures of several of hydrocarbons and an oxygen compound exist as indicated. (For interpretation of the references to colour in this figure legend, the reader is referred to the web version of this article.)

and beyond 65°N and 65°S). We here add the new calibrated and processed data from 2017.

In our previous papers, as well as in those of other investigators, it has been discussed how as the southern hemisphere moved into autumn after the mid-2009 equinox, large temperature variations were observed near the south pole (beyond 60°S) in the stratosphere (essentially from 0.1 down to 1 mbar). Indeed, while a moderate warming was observed in the summer-entering north for the mid and high northern latitudes, a spectacular drop in temperature by as much as 25 K at 70°S was measured from 2012 to 2014 in the stratosphere of Titan at levels around 0.3 mbar (Coustenis et al., 2016). Since 2014, we had no high-resolution nadir data in FP3 and FP4 to exploit for temperature and composition of the south pole, which now is feasible with the 2017 measurements. The previous temperature variations were accompanied by a strong enhancement of chemical compounds in the south polar region, while the north failed to show the opposite effect in a similar magnitude, which indicated a non-symmetrical reaction to the seasonal influence for each pole. In our 2018 paper, we showed how the north polar stratosphere only responded with a decrease of the chemical content after 2015, a three-year delay with respect to the increasing south. We explore here more recent dates seeking to determine longer-term seasonal effects near Titan's poles by the use of the 2017 observations.

3.1. Thermal structure variations in the stratosphere near the poles from 2012 to 2017

In order to determine which atmospheric levels our results pertain to, we have calculated and show in Fig. 4 the contribution functions for the methane (and hence for the temperature retrievals) and for the other molecules investigated in this paper from 2010 to 2017. Our contribution functions up to that time indicate that the emission observed in the 7.7-micron methane band (observed in CIRS FP4 from 1250 to 1350 cm^{-1} roughly when the P and R branches are taken into account and centered at 1304 cm^{-1}) originate essentially and in general from levels 0.01–20 mbar (70–400 km in altitude: Fig. 5a,b).

Our contribution functions for the southern latitudes (Fig. 4, two left columns) from the methane emission in the Q-branch and its wings indicate that at 70°S the emission in the methane band sounds pressure layers around 0.4 mbar (180 km) for the earlier dates and higher levels 0.2 to 0.02 mbar, peaking at around 0.05 mbar (300 km) in 2017. Indeed, the south polar temperature structure (Fig. 5a) shifts the contribution function upwards so that much of the temperature sensitivity is at about 0.05 mbar, but the line wings are still sensitive to the temperatures down to the 10-mbar level (Fig. 4).

On the other hand, for the northern pole, the profiles we infer correspond to pressure levels between 0.01 and 10 mbar, with weak variations with time, as supported by the small changes found in the north pole temperature structure in the recent years (Fig. 5b). The peak of the contribution functions in the north indicates sounded levels around 0.1 mbar (0.05–1 mbar: 150–300 km), close to the part of the atmosphere corresponding to the more recent southern profiles.

For the other gaseous species, the emission of the trace gases close to the south pole originates from around 10 mbar but also from higher atmospheric levels around 0.5 mbar. The northern observations on the other hand probe similar altitudes /pressure levels in the recent years, somewhat higher than for the southern latitudes, depending on the molecule as shown in Fig. 4.

In Fig. 5 we then show the stratospheric temperature on Titan beyond 65°S for different years in different colors from 2010 to 2017 and similarly poleward of 65°N and different colors for different dates from 2013 to 2017, comparing the temperature profiles inferred in this study from 2017 data with previous inferences (Coustenis et al., 2018) to derive a description of the thermal evolution in the last 7 years of the Cassini mission.

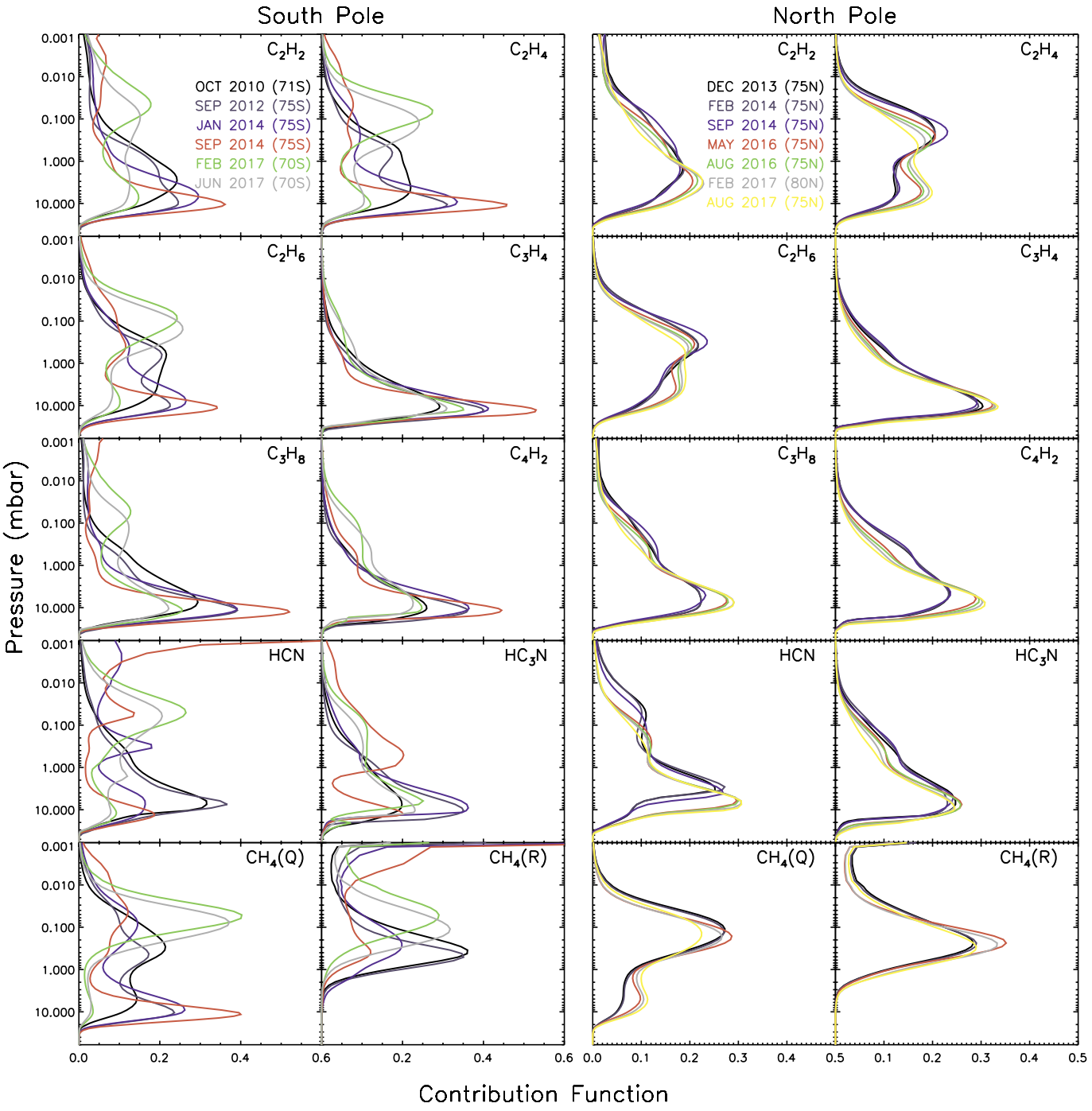

Fig. 4. Contribution functions for the species observed in Titan's stratosphere near the South Pole (left two columns) and the North Pole (right two columns). Lower four cells: contribution functions for the emission observed in the methane band in FP4 centered at 1305 cm^{-1} (Q-branch) and in the R branch (1250 cm^{-1}). The dates are given in the upper panels. For the corresponding altitude levels see Fig. 5. (For interpretation of the references to colour in this figure legend, the reader is referred to the web version of this article.)

3.1.1. Temperature evolution near the southern pole

Starting with the southern latitudes, we have previously reported on the dramatic temperature decrease from 2010 to 2014 by > 40 K at the 0.5 mbar (starting from around 170 K) and the related consequences on the gaseous abundances (Coustenis et al., 2016, 2018). We recall that after mid-2014 and until 2017 no nadir high-resolution CIRS data for the south pole were available in FP3 and FP4, highlighting the importance of the new 2017 data that we examine here. As can be seen in Fig. 5a, the temperature profiles that we have retrieved from the 2017 February and June 70°S observations, probing essentially levels around 0.05 mbar (0.02 and 0.2 mbar), are very different in shape from the previous inferences, which showed a rather homogeneous to a small positive slope with pressure in the stratospheric temperature distribution until 2014. The new profiles significantly accentuate the trend with a much steeper positive slope in the stratosphere above about 150 km ($p < 1$ mbar) and up to 300 km (0.05 mbar). The lower-altitude parts of the high south temperatures for February 2017 (Fig. 5a, black line) are located between the 2013 and 2014 ones we have previously derived up to 0.5 mbar and even the June 2017 profile (Fig. 5b, red line) rests within the values reported after 2012 up to about 0.2 mbar.

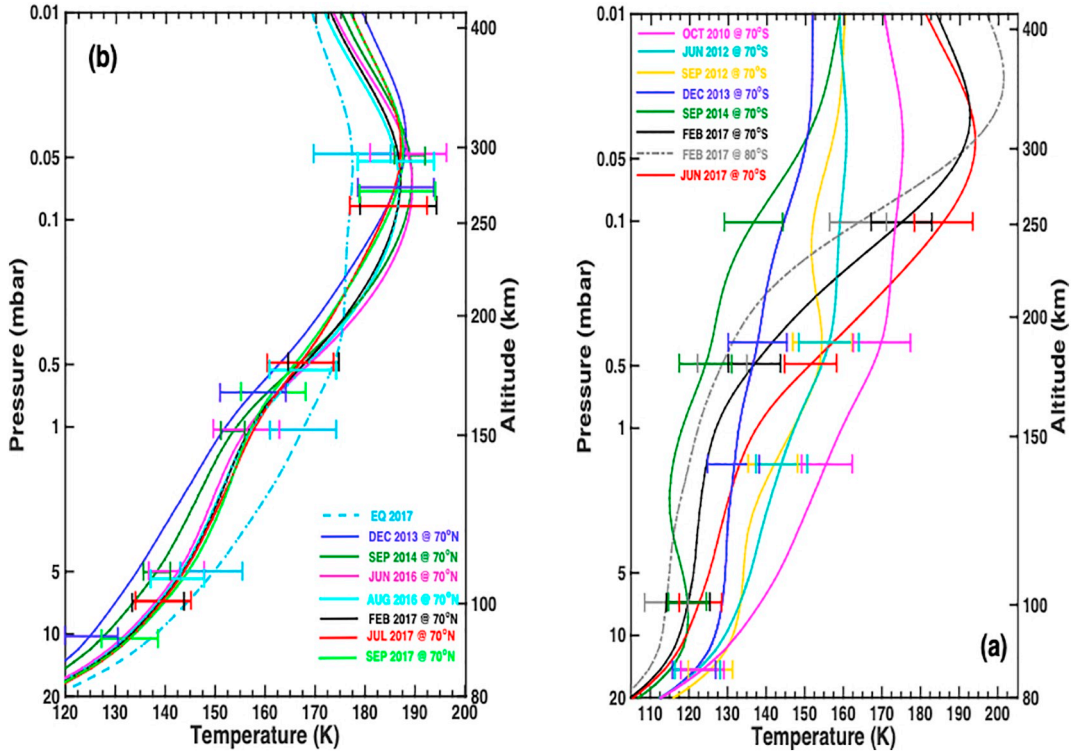

Fig. 5. Temperature evolution in Titan's stratosphere: a) near the south pole from 2010 to 2017; b): from end of 2013 to 2017 near the north pole. The different dates are indicated in different colors. The averaged equatorial thermal profile for 2017 is also plotted in dotted lines in (b). 3-σ uncertainties on the temperatures are shown with the horizontal bars at different pressure levels for clarity. (For interpretation of the references to colour in this figure legend, the reader is referred to the web version of this article.)

However, it must be noted that, taking into account the steeper-slopes of the 2017 profiles and the higher altitude levels probed in the southern data, we find higher temperatures at 70°S than previously reported and on average, the south pole appears to be returning to the warmer values found in 2010 and perhaps even more. Between February and June 2017, the Titan stratosphere gains about 15 K in the 0.5 mbar to 0.1 mbar region. Titan's southern polar stratosphere 2017 data indicate that the temperature is fast increasing above 0.5 mbar, and has gained at least 35 K with respect to 2014 up to 0.1 mbar, while in June 2017, the increase is even more impressive with temperatures attaining 150 K around 0.5 mbar and even joining or exceeding the thermal values of the northern polar region above 0.1 mbar, arriving at 190 K. Such temperatures in the higher stratosphere are now warmer than even in 2010 by 15 K or more. After a gap of about 2.5 years, the thermal increase in the south represents about +5 K in February 2017 to +30 K in June 2017 with respect to the September 2014 values.

Therefore, the stratosphere over the south pole of Titan shows dramatic increase in temperature in 2017 since 2014, by 10–50 K in the 0.5 mbar–0.05 mbar pressure range, the larger 2017 temperatures observed in the higher atmospheric levels around 0.05 mbar. Achterberg et al. (2019, in preparation) also report a noticeable warming of the south polar upper stratosphere ($p < \sim 0.5$ mbar) sometime between 2014 and 2016 using the temperature cross-sections from all the post-equinox Titan flybys with mid-infrared maps that step across multiple latitudes with N/S to Saturn oriented focal planes (MIRTMAP) covering both poles.

As shown in Fig. 5a, the February 2017 data near the south pole could afford us two different selections (this is the only occasion where we could recover enough spectra to make averages with sufficient signal-to-noise, from 65 to 70°S or from 70°S to 90°S) and we derived two different profiles centered at 70°S and 80°S (Table 1 and grey and black lines in Fig. 5a) which show the 80°S being about 10 K colder than the 70°S at around 0.5 mbar. The difference between the two retrieved profiles is due mostly to latitudinal temperature gradients, the higher southern latitudes (i.e. closer to the South Pole) remaining colder than the lower ones. If this is true, the difference between the temperature profiles for the large averages of February and June 2017, could also possibly be due at least partly to looking at slightly different latitudes, rather than reflecting temporal changes over 4 months.

3.1.2. *Temperature evolution near the northern pole*

Turning to the northern pole and comparing our new data with the earlier dates at 70°N in Fig. 5b, we still find relatively moderate changes. We had previously reported a 10 K increase from 2013 to 2016 (Coustenis et al., 2018), the north polar region's temperature starting to show an increase in reaction to the augmented sunlight as the north moves towards summer with a three-year delay with respect to the southern pole. Our 2017 temperature profile is very similar to the 2016 one in shape and values and confirm that Titan's stratosphere has become warmer by up to 10 K in the 0.05–1 mbar range, but given the uncertainties the changes could be much smaller. At lower pressure levels (altitudes higher than 250 km), the 2017 profiles seem to be a little colder than during the 2013–2014 period, but all in all and within error bars the 2016 and 2017 profiles are very similar and up to 10 K warmer than the earlier years (2013–2014) at around 1 mbar.

3.1.3. *Titan's thermal structure at the poles*

The two Titan poles then do not appear symmetrical in thermal response in the stratosphere (Coustenis et al., 2018, and Fig. 5 here) in view of the dramatic decrease in the stratospheric temperature in the south being initiated as early as 2012 (Coustenis et al., 2016). Our temperature profiles are quite compatible with the results of limb observations at various dates published by Teanby et al. (2017) for high southern latitudes and who also report on the post-equinox (after 2010) hot spot found in Titan's upper stratosphere and the ensuing large compositional enrichment over the following years and the associated

thermal cooling as we have done in previous publications. These authors find that the middle stratosphere and lower-stratosphere of Titan (around 200 km) above 80°S has gradually cooled from 170 K in 2010 to 130 K in 2015. This is remarkably consistent within uncertainties (both due to measurements and to spatial differences) with our results from Coustenis et al. (2016, 2018) as shown in Fig. 5 where also our temperatures for high southern latitudes in 2010 start from around 170 K at those altitudes and finishes at around 125 K in September 2014 (our last observation date before 2017). Teanby et al. (2017) also describe temperature changes at higher altitudes, around 400 km, with an initial warming up to 180 K in late 2011 at 80°S (we find temperatures around 170 K in late 2010), which drops by about 25 K by early 2015 (we reported a cooling down to about 155 K in September 2014). Teanby and colleagues report a heating up again at these higher levels by late 2015, while the lower stratosphere remains stable and colder at around 125–130 K. This is in agreement with our findings.

3.1.4. Temperature evolution near the equator

We finally looked at the thermal structure near the equator from a large average of 2017 data in the −10 to +10 latitudes (Table 1). Consistently with previous findings, the temperature profile for the equator is more homogeneous with altitude and similar in shape to the earlier southern profiles (e.g. June 2012), albeit considerably hotter at $p > \sim 0.5$ mbar, increasing with altitude and situated around 170 K at $p < \sim$ 0.5 mbar. Comparing this temperature profile in the 0.01–10 mbar range with the one derived from 2004 to 2005 averages at 5°S and shown Fig. 4 of Coustenis et al. (2007), we find a very clear stability of the equatorial thermal structure over the mission duration with temperatures around an average of 170 K in that pressure range.

3.2. Variations of the chemical composition in the stratosphere near the poles from 2012 to 2017

It has been previously shown that as seasosl shift on Titan, the strong changes witnessed in temperature near Titan's poles, are usually accompanied by a decrease or an increase in radiative emitters. The latter has already been observed and reported previously for somewhat lower latitudes, for instance around 50°N, a latitude located at the border of the northern vortex. As indicated in previous publications from CIRS data (e.g. Teanby et al., 2012; Vinatier et al., 2015; Coustenis et al., 2018), temperature and composition changes took place essentially in the south pole in these past years, with a strong enhancement observed for several of the species in the atmosphere as the southern pole entered into autumn after 2010. Indeed, a couple of years after Titan's northern spring equinox in mid-2009, the stratospheric dynamics on Titan featured a global reversal as the south pole was entering fall, leading to a substantial enrichment of the trace gases within the southern pole vortex created by subsidence from 2012 onwards. According to current General Circulation Model models, this single circulation cell pattern should persist until 2025.

While the northern winter vortex was shown to be weakening and finally disappeared in the past years (Coustenis et al., 2013; Jennings et al., 2015; Teanby et al., 2017), the nadir temperature data from the 3 cm^{-1} temperature maps shows that the southern vortex became broader sometime between late 2014 and late 2016: the peak wind velocity and temperature gradient shifted from 70S to ~45S, but the maximum wind velocity remained about the same or slightly lower (Achterberg et al., 2019, in preparation). The results by Teanby et al. (2017) from 2015 and 2016 measurements suggest a small decrease of gases at the highest altitudes due to this broadening of the south polar vortex and to the dilution of the enriched gas. The trace gas retrievals here then agree in indicating a weakening of the subsidence in later dates.

Indeed, as we had no exploitable high-resolution nadir FP3 and FP4 data between late 2014 and 2017, we find here that the strong increase in temperature over the south pole in 2017 with respect to 2014 is associated with a significant and rapid drop in chemical content near the south pole (Fig. 6). We thus witness in Titan's south pole the negative evolution or even disappearance of several trace species, such as HC_3N and C_6H_6, previously observed clearly at high southern latitudes (for a precise description of the lifetimes of the gaseous species in Titan's stratosphere see Section 4 of Coustenis et al., 2016). This is due to the seasonal change on Titan, moving from northern winter in 2004 to advanced northern spring in 2012 and towards summer solstice in mid-2017, with the opposite effect in the south pole as it moves into winter. The effect of this seasonal evolution is predicted to be a reversal of the circulation cell allowing for gaseous components to move from the equator to the South (see e.g. Teanby et al., 2012).

Fig. 6 shows our findings for the abundances of the minor gaseous components near both poles, with a maximum of the contribution functions in the 0.1–10 mbar range (90–250 km). We have omitted CO_2, which shows no significant variations in 2017. The blue lines in Fig. 6 represent the south polar latitudes around 70°S and show increase in the abundances by one or several orders of magnitude for many gases until the end of 2014, as described in Coustenis et al. (2018).

First, we compare our 2017 equatorial gaseous abundances (green points in Fig. 6), with those we have measured during the Cassini mission starting almost two seasons earlier (e.g. Coustenis et al., 2007, 2010; Bampasidis et al., 2012; Vinatier et al., 2015; Vinatier et al., 2018). In 2017, the data provide only an upper limit in C_6H_6 abundance of about 1×10^{-10}, which is comparable to values of about $1–2 \times 10^{-10}$ found throughout the mission, when the benzene signature was detectable. Similarly, for HC_3N, its abundance is about 10^{-10} in 2017 and varies from 1 to 3 times that value throughout the mission, when appearing. CO_2 has been quite constant at equatorial latitudes in the past 13 years and the value found in 2017 ($1.5\ 10^{-8} \pm 0.5\ 10^{-8}$) is very close to the one reported in 2004, as it is also quite compatible with the values reporter at higher latitudes. The same applies for C_2H_2, C_2H_4, C_2H_6, C_3H_4 and C_4H_2, which have remained close to values of about 3×10^{-6}, 10^{-7}, 8×10^{-6} and 5×10^{-9}, and 1.2×10^{-9}. Only HCN and C_3H_8 show a deviation from their 2004 values here. Propane seems to have increased in the past 13 years with more recent equatorial values consistently being 2–3 times higher than at the beginning of the mission. HCN on the other hand has shown some decrease in the latter season by about a factor of 2. We note that HCN and C_3H_8 are long-lived photochemical species, more potent to changes inflicted by solar cycle modulations of the incoming insolation over the 13 years of Cassini observations. Thus we believe these differences in the equatorial abundances of these species are a subtle demonstration of this effect. Photochemical models assuming solar maximum and minimum insolation demonstrate that the anticipated changes in the abundances of HCN and C_3H_8 are factors of ~2 with higher insolation resulting to increased abundances for HCN and reduced for C_3H_8 (Lavvas, 2007; Vuitton et al., 2019). The solar insolation was higher in 2004 compared to 2017 (http://lasp.colorado.edu/lisird), however the flux difference between the two years discussed here (2004, 2017) is smaller than the maximum differences occurring from solar minimum (2009–2010) to solar maximum (2014–2015). Therefore, the models appear to be qualitatively consistent with the observations, yet further evaluations of the temporal evolution of the abundances may reveal further details of the impact of the solar cycle. The Cassini observations presented here provide significant constraints for the validation of such simulations. However, on the whole, the equatorial latitudes seem to be much less affected, if at all for most molecules, by the changes in seasons.

As Fig. 6 (red lines) shows, we find that all trace gases in the Titan north polar area have decreased from September 2013 to August 2017, except for CO_2 which remains constant within error bars and is not shown on this plot. Propane (C_3H_8) has shown a trend for decrease until 2016, but from more recent data and within error bars we see no additional decrease of its abundance in 2017, where it remains at around 1.5×10^{-6}.

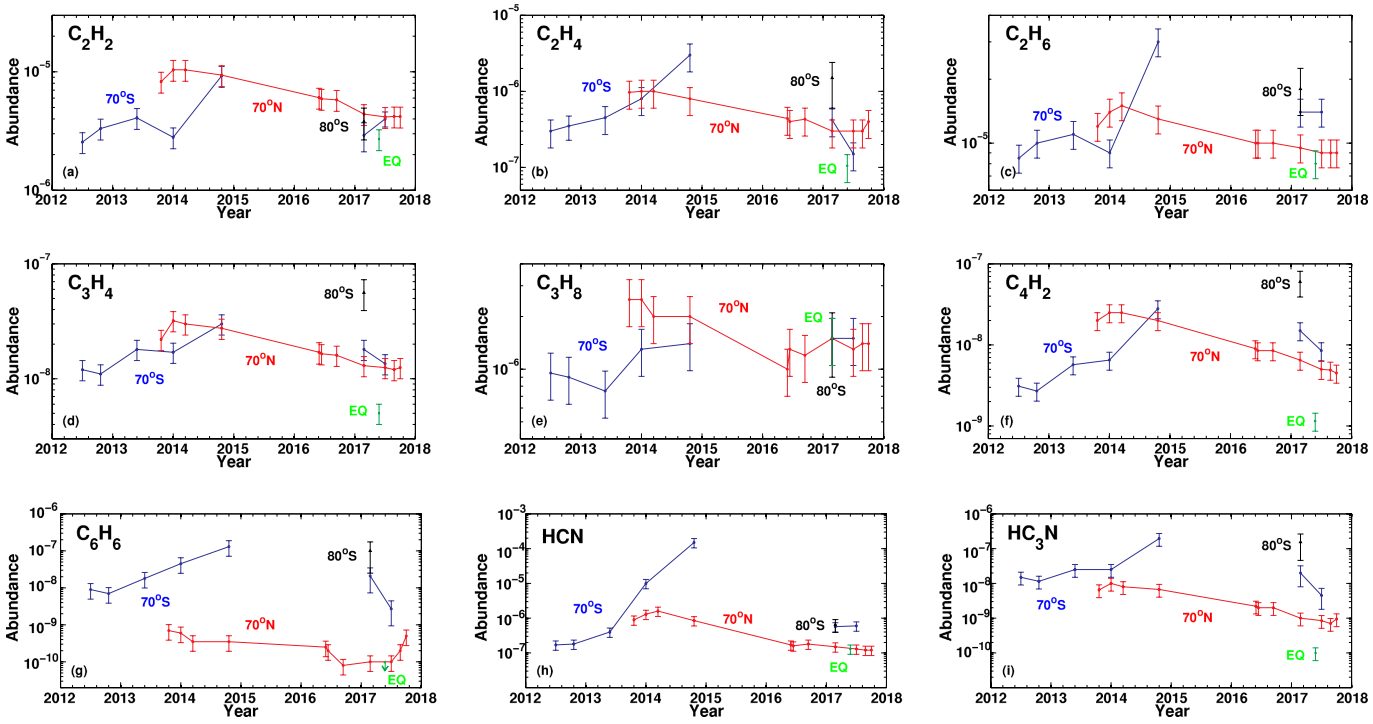

Fig. 6. : Abundances of trace hydrocarbon and nitrile gases in the stratosphere of Titan from 2012 to 2017 for the south polar region near 70°S (blue lines) and some exceptional data taken near 80°S in February 2017 (black points), for the north polar region (red lines-near 70°N) and an equatorial average in 2017 from −10° to +10° as green points. Note that we have no FP3 nadir data between 2014 and 2017 for the south polar region and that therefore the connecting blue lines are not interpolated (see table for detailed description of selections). 3-sigma error bars are indicated. (For interpretation of the references to colour in this figure legend, the reader is referred to the web version of this article.)

In this 4-year period, we find the decrease we had announced in Coustenis et al. (2018) near the northern polar region to be confirmed and prolonged. In total, from the abundances around the beginning of 2014, when the north polar stratosphere was stable with enhanced species, until September 2017 (about 3 years time), we witness a drop in content of various trace gases as follows:

- C_2H_2, C_2H_6 and C_3H_4 decrease by factors of about 2–3.
- For C_2H_4 and C_4H_2 the abundances decrease by factors of about 3.5–5.
- We find HCN and HC_3N to be less abundant by more than an order of magnitude
- C_6H_6 decreased until the end of 2016, but it seems to have stabilized during the first half of 2017 at around 0.1 ppb, which is 5–7 times lower than in early 2014. Then it seems to be slightly increasing again since mid-2017, reaching similar values as 4 years ago, by the end of 2017. Although this increase appears real in view of the error bars, one should be cautious because of the difficulty in extracting the gaseous benzene contribution from the area around 674 cm^{-1}, due to the interference from other species like C_2H_2 and HCN, which have bands with strong spectroscopic signatures.

The north polar region has thus continued to become rarified in most of the stratospheric gases (exceptions are CO_2 and C_3H_8), with the hydrocarbons somewhat less affected than the nitriles HCN and HC_3N, who are reduced by more than an order of magnitude.

CO_2 and C_3H_8 find their abundances undiminished with respect to previous years in the North as for the other molecules. CO_2 is a chemical product with extremely large photochemical life time, while we do not have a clear picture of its behavior from the GCM results discussed in Section 4. C_3H_8 is one of the most abundant molecules where the abundance retrieval is complicated due to the emission signature being mixed with the C_2H_2 one, which has more emission.

In the south pole, where we had no data since 2014, and following the rapid huge enhancement of the chemical species from 2012 to 2014 (e.g. as described in Coustenis et al., 2016, 2018; Vinatier et al., 2015; Teanby et al., 2017), we now report a strong decrease. All the molecules (except for CO_2) have dropped with respect to the end-of-2014 peak at latitudes near 70°S and are now at abundance levels close to the ones witnessed in 2013 (Fig. 6, blue lines). This corresponds to the results we have in the thermal profile which, as indicated in Section 2, has returned for these southern latitudes to values close to those found at dates around 2012. We do not know if the southern latitudes abundances increased further after 2014, and when exactly the decrease began, but sometime after 2014, a significant decrease started in the south. Our two data points in 2017 (February and June at 70°S) confirm this is the case for all molecules with significant drops in mixing ratio, with the exception of C_3H_8 and CO_2, which show no real differences since 2014.

The new 2017 values indicate that since the peak found in September 2014 Titan's stratosphere above around 70°S suffered a considerable loss in abundance as follows:

- C_2H_2, C_2H_6, C_3H_4 and C_4H_2 were reduced by factors of 1.5–2.
- C_2H_4 and C_6H_6, although difficult to infer, show nevertheless very strong decrease in abundance in 2017 with a drop by one and up to two orders of magnitude respectively. The latter (C_6H_6) is currently almost showing the same value at some 10^{-9} near both poles.
- HC_3N has also lost 1.5 orders of magnitude in abundance, dropping close to its northern value of about 10^{-9}. HCN is the most dramatically affected near 70°S with its mixing ratio reduced by 2.5 orders of magnitude, down to some 6×10^{-7}, while it had reached values of about 2×10^{-4} towards the end of 2014.

As said above, we had the opportunity in February 2017 to recover another average of spectra at even higher latitudes centered around

80°S (as described in Table 1). The analysis of this dataset is shown with black points in Fig. 6. In all cases the spectral averages closer to the southern pole on that specific date show higher values than the ones at 70°S. Since there is a fairly strong temperature gradient with hotter temperatures between 60° and 90°S in the upper stratosphere, the differences in abundances could be due to these discrepancies tied with the temperature changes described in Section 3.1. This again points to the possibility that the southern stratosphere closer to the pole maintains some of the larger abundances and it has not lost as much of its content as the lower latitudes. The decrease in chemical species might then be affecting first lower latitudes before reaching the pole.

We have to note again that we do not know if these decreases are the largest that affected Titan's stratosphere above around 70°S, as we did not have any high-resolution FP3 nadir data between the end of 2014 and the beginning of 2017 roughly. But they bring the indication that Titan's southern polar region became subject to strong seasonal variations between autumn equinox and winter solstice, while in 2014 Titan was in the middle of autumn in the south. We have already compared our findings (as much as possible given the differences in mixing ratio inferences: constant-with-height vs vertical distributions) to the results from the analysis of high southern limb spectra up to dates in 2016 by Teanby et al. (2017), and indicated that for the dates we had previously exploited in our 2016 and 2018 papers, the abundances are very compatible for all molecules except for the nitriles where we find higher values (Coustenis et al., 2018, Section 3.2).

Other investigations, in particular using the Focal Plane 1 (FP1: 10–500 cm^{-1}) spectral part of the CIRS Titan data have also shown that the meridional distribution evolution of temperature and chemical composition from northern winter (2004) to summer solstice (2017) denote important seasonal changes in the lower stratosphere (between 10 and 20 mbar). This is especially true, as reported from these mid-infrared analyses at the South pole (close to 70°S), where temperature decreased by 24 K at 6 mbar and by 19 K at 15 mbar within 4 years from 2012 onwards (Sylvestre et al., 2018, 2019).

Teanby et al. (2018) present an analysis of data acquired with ALMA in March 2017, and among other they present profiles for C_3H_4 extracted from a Titan disk-average spectrum. Since in 2017 we find the northern and the southern constant-with-height mixing ratios of C_3H_4 (Fig. 6) to be quite similar with values around 10^{-8}, we deduce a compatibility with the results of Teanby et al., who have a similar average value in their two-point profile from 100 to 300 km in altitude around and a somewhat lower abundance in their uniform profile. These results confirm the moderate decrease in abundance for methylacetylene since the end of 2014 in the south compared to the decrease in other molecules, also noted by Teanby et al. (2018) who point at the similarities with the values from Vinatier et al. (2015). Our error bars in Fig. 6 indeed show that the 2017 C_3H_4 abundances can be compatible with the values in the period 2014–2015.

4. Conclusions and interpretations

We discuss here the global picture of seasonal temperature and chemical composition variations in the stratosphere near Titan's poles from 2010 to 2017, while Titan moved from northern winter in 2004 to advanced northern spring in 2012 and towards summer solstice in mid-2017, with the opposite effect in the south pole as it moves towards winter. During that time, Titan's main atmospheric circulation cell is expected to reverse and models predict that newly produced photochemical species are channeled from mid latitudes towards the south pole (e.g. Teanby et al., 2012). Where we have data, we searched for signatures of trace stratospheric gases in large spectral averages around the poles and determined their abundances.

Our previous results had shown that the southern pole of Titan became substantially enhanced in trace gases after 2012 and has dramatically decreased in temperature in 2012–2014 (Fig. 5). The situation has reversed in 2017 with the temperatures increasing and the chemical content decreasing, as also witnessed in medium-resolution data (Achterberg et al., 2019, in preparation). In the North, we had found that the composition decrease expected to compensate for the strong enhancement in the South only set in about 3 years after the south had begun to become enriched (roughly 2015 vs 2012) and continues in 2017.

The general characteristics of our temperature and composition retrievals in this period (as found also by other investigators, e.g. Vinatier et al., 2015) are in agreement with the broad features of Titan's atmospheric circulation derived by GCM models (Lebonnois et al., 2009). These results demonstrate that between vernal equinox and summer solstice the circulation pattern changes from a two-shell circulation with upwelling at the equator and descending at the poles, to one global shell circulation ascending from the summer pole and descending to the winter pole. The transition period between these two patterns is 3 terrestrial years which means that by the end of 2012 a global pole to pole circulation is established. This is the time when the increase in the south pole abundances is observed. However, the latest south pole observations from 2017 reveal a different trend in both temperature and composition from that established up to 2014. As shown in Fig. 6, in the past years we see in the southern polar region the gradual but rapid decrease to almost disappearance of several trace species among the complex hydrocarbons and nitriles, previously notoriously found there. This is associated to a remarkable increase in temperature at the south pole in 2017 as compared to 2014 (Fig. 5a). As the species with the strongest drop in abundance are important infrared emitters, the correlation with the increase in temperature is consistent with theoretical anticipations (Teanby et al., 2017). On the contrary, the north pole becomes increasingly rarefied while its temperatures present smaller variations warming by about 5–10 K near 1 mbar.

We can compare the general picture of Titan's seasonal changes observed with CIRS to the corresponding evolution of polar temperature and composition from the Titan GCM database that describes a coupled picture of circulation, photochemistry and haze microphysics (Rannou et al., 2005). We note that the GCM results discussed hereafter were derived based on pre-Cassini data, thus have not benefited to any degree from the plethora of new observational constraints as well as the improvements that the new constraints have induced on our understanding of the physical and chemical processes in Titan's atmosphere over the last 15 years. As noted in most recent publications concerning GCM models for Titan's atmosphere (e.g. Lebonnois et al., 2012; Lora et al., 2015), there is no complete study of the predictions on the seasonal variations of the Titan chemical composition in the stratosphere. Thus, our goal with this comparison is to highlight the aspects that need to be improved in the future applications of GCM models, based on the Cassini CIRS observations.

In Fig. 7 we present the seasonal evolution of the mixing ratios over the polar regions normalized to the 2010 and 2013 observations for the South and North pole, respectively. We resolve to this relative comparison and not to a direct comparison of mixing ratios in order to focus on the impact of the dynamics on the chemical composition. According to the GCM simulations the polar abundances depend on the interplay between the influx of photochemical products in the winter polar region by the Hadley cell, and the loss of these species in the lower stratosphere due to condensation, while chemical effects have a secondary role in the resulting temporal evolution of the chemical abundances (Hourdin et al., 2004). As seasons change the advection of material to the poles, as well as, the thermal structure (therefore the condensation rates) change, resulting to different polar enhancements. The atmospheric location probed for each species (contribution function) further affects the degree of temporal variation observed over the seasons. Therefore, we used the contribution function derived in our studies over different times (see Fig. 4) as a reference time-grid on which we interpolate to derive the contribution function for each species at the reference times of the GCM database (resolution of ~1 Earth year). With these contribution functions we calculate the average

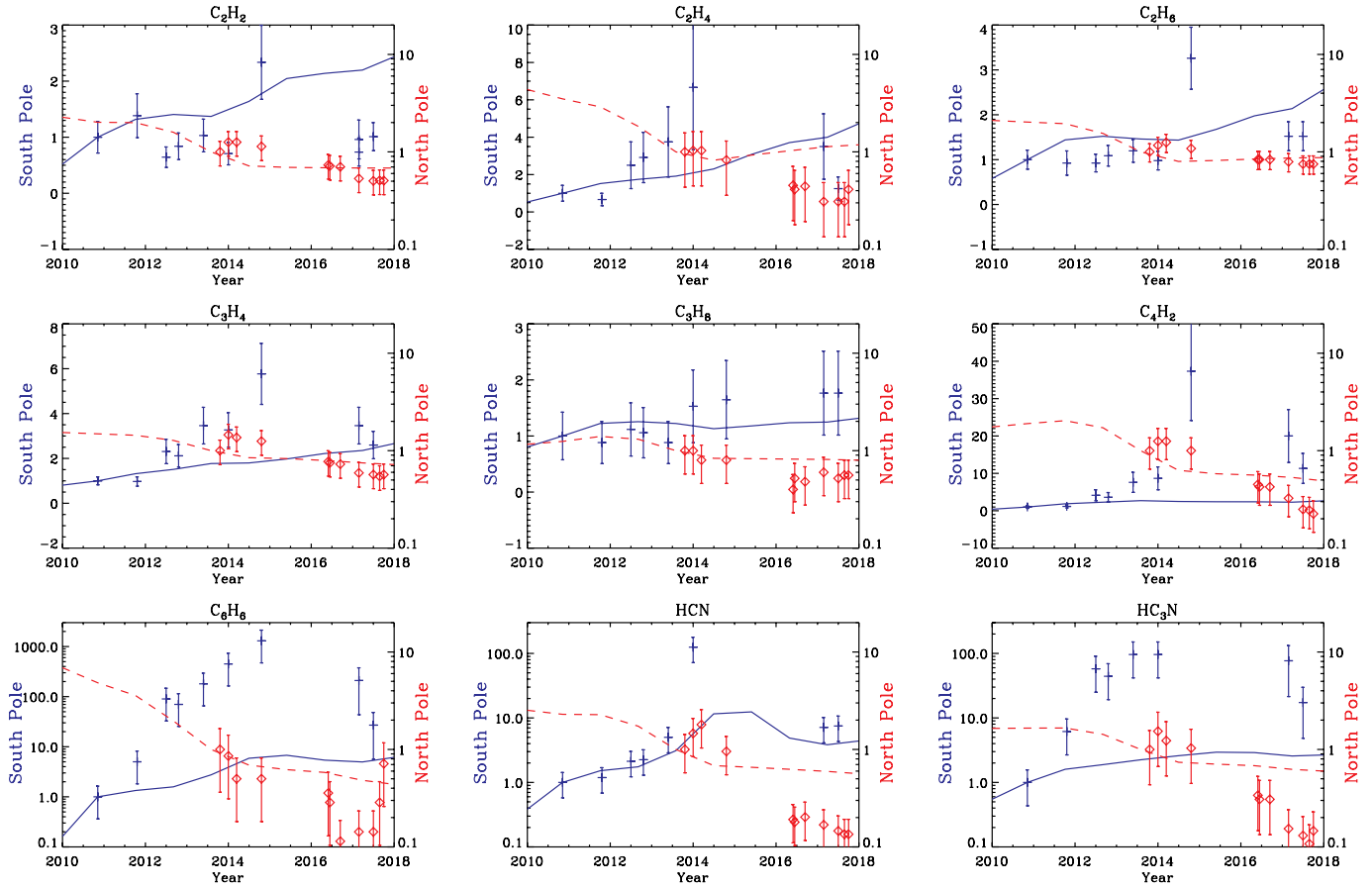

Fig. 7. : Seasonal evolution of the mixing ratios over the polar regions normalized to the 2010 and 2013 observations for the South (in blue) and North (in red) pole, respectively. Symbols with error bars present the CIRS observations and lines the GCM simulations (database by Rannou et al., 2005). The scale on the left is the ratio of mixing ratios x(t)/x(2010) for the south pole (blue curves/points) and the scale on the right the corresponding ratio x(t)/x(2013) for the north pole (red). (For interpretation of the references to colour in this figure legend, the reader is referred to the web version of this article.)

mixing ratio of each species for all simulated profiles within the latitude grid of 70 and 90° for each pole.

The observed abundance ratios demonstrate that in the south pole C_2H_2, C_2H_6, and C_3H_8 remain approximately constant or slightly increase by factors < 2 within error bars over the period 2010–2017, with the exception of the latest observation in 2014 that reveals an enhancement particularly for C_2H_6 up to a factor of 3 relative to the 2010 abundance. For C_2H_4, C_3H_4, and C_4H_2 the increase of their abundances towards 2014 is more pronounced starting from 2012 and reaching maximum values of ~6 for C_2H_4 and C_3H_4, while C_4H_2 increases by a factor of ~40 by 2014. Similarly, the 2017 observations reveal a clear decrease in the abundances of these species, with C_2H_4 reaching the 2010 abundance, while C_3H_4 and C_4H_2 are dropping at about 2 times and 10 times the 2010 abundance. For C_6H_6, HCN and HC_3N the observations reveal the maximum effect of seasonal changes, with the 2014 ratios reaching values of ~100 for HCN and HC_3N, and ~2000 for benzene, while the rate of increase is strongest for C_6H_6 and HC_3N, which by mid-2012 reveal enhancement factors of ~50–100 relative to the 2010 abundances. As with the other species, the abundance ratios drop in 2017, but still remain higher by factors of ~8 (HCN), 20 (HC_3N), and 30 (C_6H_6) in August of 2017 relative to 2010. Over the north pole, observations between 2014 and 2017 reveal a consistent decrease in abundances by factors ranging between 1 and 10, while as with the south pole HCN, HC_3N, and C_6H_6 demonstrate the strongest temporal variations.

When compared to the GCM results (Rannou et al., 2005), we find that the simulated circulation provides a global picture that is consistent with the observations. The magnitude of temporal variation observed for the various species is consistent with the anticipations based on the correlation with their condensation level. Estimates for the altitudes where different species should condense in Titan's atmosphere demonstrate that C_2H_2, C_2H_4, C_2H_6, C_3H_4, and C_3H_8 condense at similar altitudes below 60 km, HCN, HC_3N, and C_4H_2 near 75 km, while C_6H_6 near 85 km (see Fig. 1 in Lavvas et al., 2011). Although these altitudes correspond to equatorial temperature conditions, the grouping of species will remain similar at different temperatures, as their saturation vapor pressures dominantly control their condensation levels. Thus, species within each of the above groups should demonstrate similar magnitude temporal variations, as our observations reveal. However, there are subtle details not yet captured by the models. Over the south pole and for most of the species, the temporal variation of the mixing ratios is consistent with the observations, when these are of small (C_2H_2, C_2H_4, C_2H_6, C_3H_8) or moderate (C_3H_4, C_4H_2) magnitude, but the model fails to capture the increase observed around 2014, as well as, the drop following it. The simulations provide a better description for the HCN temporal variation capturing the increase in the abundance towards 2014 and the subsequent drop with remarkable agreement in the magnitude, except at the peak value seen at the end of 2014 for which the model is lower than the observation by a factor of ~10. For the other species demonstrating a strong temporal variation (HC_3N, C_6H_6), the simulations do not capture the observed strong enhancement or even the temporal variation. Over the north pole, the simulations capture the common characteristic of abundance reduction (with the exception of C_2H_4), and provide results consistent with the observations of C_2H_2, C_2H_6, C_3H_4 and C_3H_8. However, for higher order hydrocarbons the observed reduction in mixing ratios in 2016 and 2017 is higher than

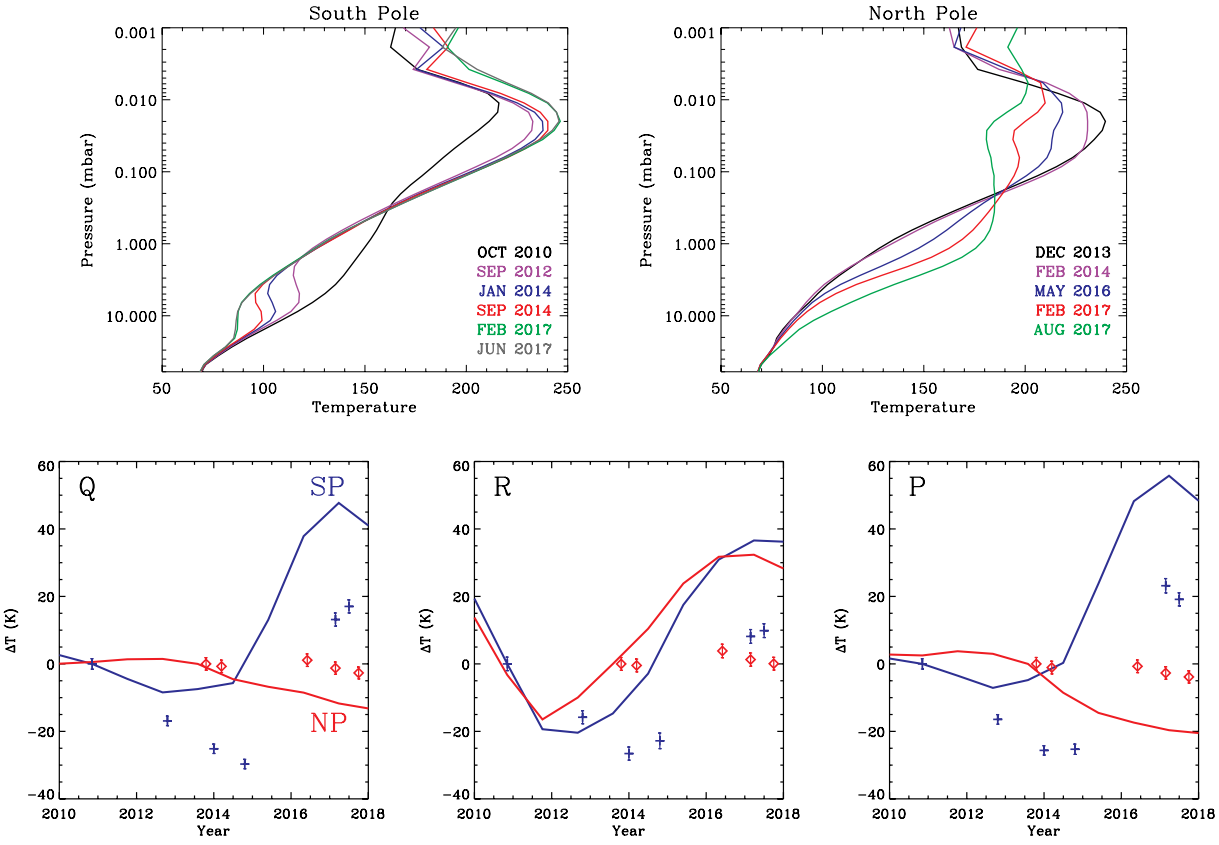

Fig. 8. (upper panel): temporal evolution of the thermal structure as found by GCM models; (lower panel): comparison between the CIRS observations acquired at the dates shown in the upper panel and the temporal differences in the average temperatures calculated with the contribution functions of the methane band Q, R and P branches. (For interpretation of the references to colour in this figure legend, the reader is referred to the web version of this article.)

the GCM simulations.

We can further compare the temporal evolution of the thermal structure from observations and models (Fig. 8 upper panel). At the south pole the GCM suggests a continuous temperature increase that reaches its maximum early in 2017 in the upper atmosphere, while the opposite behavior is observed in the lower stratosphere. At the north pole, the upper stratosphere progressively cools beyond 2013, reaching a quasi-isothermal profile above ~1 bar in August 2017, while at higher pressures the opposite behavior of temperature rise is expected. Although these general characteristics are consistent with the observations their magnitude is different. The upper stratosphere of the south pole first passes through a temporal temperature decrease between June 2012 and at least September 2014, before increasing again towards the temperature maximum observed in 2017 (see Fig. 5a). This different behavior relative to the models has also been seen in CIRS limb observations (Teanby et al., 2017). At higher pressures, model and observations have a similar temporal discrepancy as at lower pressures, but the general behavior of the simulations is more consistent with the observations.

These differences can be better demonstrated when comparing the temporal variations in the average temperatures calculated over the full width at half maximum (FWHM) of the contribution functions of the CH_4 Q, R and P branches (Fig. 8 lower panel). As shown in Fig. 4, each CH_4 branch is sensitive to different parts of the atmosphere that varies with time. For the Q and P branches (the P branch not shown in Fig. 4 has a similar behavior to the Q branch), the contribution functions have two broad peaks in the middle and lower stratosphere in 2010 and progressively shift towards a single peak probing at 10 mbar by the end of 2014. However, the situation reflexes in 2017 with the Q and P branches probing mainly the upper stratosphere near 0.05 mbar. Therefore, based on the observed temperature profiles, the average temperature changes (relative to 2010) are negative until 2014 when the temperature in the lower atmosphere drops in the south pole, and positive in 2017 as the temperature in the upper stratosphere is higher relative to 2010. The corresponding GCM average temperature differences do follow this behavior but with a different magnitude. The temperature drop between 2010 and 2014 is smaller than the observed and reaches a maximum of ~−10 K in mid 2012, while the temperature rise in the upper atmosphere with a maximum in 2017 is ~50 K, i.e. more than a factor of 2 larger than the observed. For the R branch the contribution function peaks near 0.5 mbar in 2010 and progressively moves to lower pressures reaching to ~0.05 mbar in 2017. Thus, observations demonstrate a negative temperature difference relative to the 2010 that decreases after 2014 but remains at negative values up to 2017. The corresponding average temperature changes for the GCM are more symmetric and demonstrate a rapid increase in temperature after 2013 reaching to +35 K by mid-2017.

At the north pole the contribution functions indicate a more stable with time variation. The Q and P branches have a dominant contribution at 0.1 mbar and a secondary near 5 mbar, while the R branch has a single broad profile centered at ~0.2 mbar. As our retrieved north pole temperature profiles are similar over the period under investigation the derived average temperatures are very close thus resulting to small temperature differences. Although the simulations do demonstrate a smaller temperature change in the north relative to the south pole, the simulated temperature decrease is stronger than the observations for the Q and P branches, while for the R branch temperature rises by about 30 K although the observations suggest temperature differences smaller than 5 K over the observed period.

Along with the gases the circulation also enhances the haze abundance in the winter pole, which has further implications for the thermal structure. Haze particles can locally cool the atmosphere, and due to the

lack of solar radiation this effect will be more important relative to lower latitudes where heating by absorption of solar light balances the cooling. This mechanism could be relevant for the stronger temperature gradient observed in the 2017 temperature retrievals if the haze accumulation is higher at that time in the lower stratosphere.

In summary, our report here takes into account the whole pool of nadir high-resolution CIRS polar spectra to the end of the mission in 2017 and aims to bring improved understanding of the seasonal and temporal evolution of Titan's complex atmospheric system. We show strong variations in the thermal and chemical structure of Titan near the south pole and significant ones near the northern pole as they evolve seasonally, while the equatorial latitudes remain rather unaffected throughout the Cassini mission. Using the very last data from Cassini, we set constraints on photochemical and circulation models, which need to account for the asymmetry found in the poles' behavior. A future space mission to Titan's complex system will have to complement the important findings of the highly successful Cassini-Huygens mission and bring answers to the many new questions it has raised, in particular concerning the organic chemistry and its evolution with time.

We have shown that the south pole of Titan is now losing its strong enhancement, while the north pole also slowly continues its decrease in gaseous opacities and has not picked up again. It would have been interesting to see when this might happen, but the Cassini mission ended in September 2017. Perhaps future ground-based measurements and future space missions can pursue this investigation and monitor Titan's atmosphere to characterize the seasonal events.

Acknowledgements

The authors acknowledge support from NASA's Cassini mission and Cassini data Analysis program, as well as from the French Centre National d'Etudes Spatiales.

References

Achterberg, R.K., Conrath, B.J., Gierasch, P.J., Flasar, F.M., Nixon, C.A., 2008. Titan's middle-atmospheric temperatures and dynamics observed by the Cassini composite infrared spectrometer. Icarus 194, 263–277.

Achterberg, R.K., Gierasch, P.J., Conrath, B.J., Flasar, F.M., Nixon, C.A., 2011. Temporal variations of Titan's middle-atmospheric temperatures from 2004 to 2009 observed by Cassini/CIRS. Icarus 211, 686–698.

Bampasidis, G., et al., 2012. Thermal and chemical structure variations in Titan's stratosphere during the Cassini mission. Astrophys. J. 760 (2) (8 pp 144).

Conrath, B.J., Gierasch, P.J., Ustinov, E.A., 1998. Thermal structure and Para hydrogen fraction on the outer planets from Voyager IRIS measurements. Icarus 135, 501–517.

Coustenis, A., et al., 2007. The composition of Titan's stratosphere from Cassini/CIRS mid-infrared spectra. Icarus 189, 35–62.

Coustenis, A., et al., 2010. Titan trace gaseous composition from CIRS at the end of the Cassini–Huygens prime mission. Icarus 207, 461–476.

Coustenis, A., et al., 2013. Evolution of the stratospheric temperature and chemical composition over one Titanian year. Astrophys. J. 779, 177 (9 pp).

Coustenis, A., et al., 2016. Titan's temporal evolution in stratospheric trace gases near the poles. Icarus 270, 409–420.

Coustenis, A., et al., 2018. Seasonal evolution of Titan's stratosphere near the poles. Astrophys. J. Lett. 854, L30 (7 pp).

Flasar, F.M., et al., 2004. Exploring the Saturn system in the thermal infrared: the composite infrared spectrometer. Space Sci. Rev. 115, 169–297.

Flasar, F.M., et al., 2005. Titan's atmospheric temperatures, winds, and composition. Science 308, 975–978.

Hourdin, F., Lebonnois, S., Luz, D., Rannou, P., 2004. Titan's stratospheric composition driven by condensation and dynamics. J. Geophys. Res. 109 (E), E12005 (15 pp).

Jennings, D.E., et al., 2012a. Seasonal disappearance of far-infrared haze in Titan's stratosphere. Astrophys. J. 754, L3 (4 pp).

Jennings, D.E., et al., 2012b. First observation in the south of Titan's far-infrared 220 cm^{-1} cloud. Astrophys. J. 761 (L15) (4 pp).

Jennings, D., et al., 2015. Evolution of the far-infrared ice cloud at Titan's south pole. Astrophys. J. 804 (L34) (5 pp).

Jennings, D.E., et al., 2017. Composite infrared spectrometer (CIRS) on Cassini. Apl. Opt 56, 5274–5294.

Lacis, A.A., Oinas, V., 1991. A description of the correlated k distribution method for modeling nongray gaseous absorption, thermal emission, and multiple scattering in vertically inhomogeneous atmospheres. J. Geophys. Res. 96 (D5), 9027–9063.

Lavvas, P., 2007. Spatial and temporal variability in Titan's atmosphere and surface: Simulation and interpretation through space and ground-based observations. PhD Thesis. Physics Department, University of Crete, Greece. https://elocus.lib.uoc.gr//dlib/8/4/4/metadata-dlib-2007lavvas.tkl.

Lavvas, P., Griffith, C.A., Yelle, R.V., 2011. Condensation in Titan's atmosphere at the Huygens landing site. Icarus 215, 732–750.

Lebonnois, S., Rannou, P., Hourdin, F., 2009. The coupling of winds, aerosols and chemistry in Titan's atmosphere. Philosoph. Trans. Royal Soc. A 367, 665–682.

Lebonnois, S., Burgalat, J., Rannou, P., Charnay, B., 2012. Titan global climate model: a new 3-dimensional version of the IPSL titan GCM. Icarus 218, 707–722.

Lora, J.M., Lunine, J.I., Russell, J.L., 2015. GCM simulations of Titan's middle and lower atmosphere and comparison to observations. Icarus 250, 516–528.

Niemann, H.B., et al., 2010. Composition of Titan's lower atmosphere and simple surface volatiles as measured by the Cassini-Huygens probe gas chromatograph mass spectrometer experiment. J. Geophys. Res. 115, E12006 (22 pp).

Nixon, C.A., Ansty, T.M., Lombardo, N.A., et al., 2019. Astroph. J. Supp. Series (in press, arXiv:1907.12612).

Rannou, P., Lebonnois, S., Hourdin, F., Luz, D., 2005. Titan atmosphere database. Adv. Space Res. 36, 2194–2198.

Sylvestre, M., Teanby, N.A., Vinatier, S., Lebonnois, S., Irwin, P.G.J., 2018. Seasonal evolution of C_2N_2, C_3H_4, and C_4H_2 abundances in Titan's lower stratosphere. Astron. Astrophys. 609 (A64) (13 pp).

Sylvestre, M., Teanby, N.A., Vatant d'Ollone, J., Vinatier, S., Bezard, B., Lebonnois, S., Irwin, P.G.J., 2019. Seasonal Evolution of Temperatures in Titan's Lower Stratosphere. (submitted).

Teanby, N.A., et al., 2012. Active upper-atmosphere chemistry and dynamics from polar circulation reversal on Titan. Nature 491, 732–735.

Teanby, N.A., Bézard, B., Vinatier, S., et al., 2017. The formation and evolution of Titan's winter polar vortex. Nature Comm 8 (1586) (13 pp).

Teanby, N.A., et al., 2018. The origin of Titan's external oxygen: further constraints from ALMA upper limits on CS and CH_2NH. Astron. J. 155 (251) (8 pp).

Vinatier, S., et al., 2015. Seasonal variations in Titan's middle atmosphere during the northern spring derived from Cassini/CIRS observations. Icarus 250, 95–115.

Vinatier, S., Schmitt, B., Bézard, B., Rannou, P., Dauphin, C., de Kok, R., Jennings, D.E., Flasar, F.M., 2018. Study of Titan's fall southern stratospheric polar cloud composition with Cassini/CIRS: detection of benzene ice. Icarus 310, 89–104.

Vuitton, V., Yelle, R.V., Klippenstein, S.J., Hörst, S.M., Lavvas, P., 2019. Simulating the density of organic species in the atmosphere of titan with a coupled ion-neutral photochemical model. Icarus 324, 120–197.

West, R.A., et al., 2011. The evolution of Titan's detached haze layer near equinox in 2009. Geophys. Res. L. 38 (L06204) (4 pp).

West, R.A., et al., 2016. Cassini imaging science subsystem observations of Titan's south polar cloud. Icarus 270, 399–408.